Journal of the American Chemical Society

An environmentally-responsive reciprocal replicating network

Craig C. Robertson,[‡] Harold W. Mackenzie,[†]
Tamara Kosikova and Douglas Philp*

School of Chemistry and EaStCHEM, University of St Andrews, North Haugh St Andrews, Fife KY16 9ST, United Kingdom

*Corresponding author e-mail: d.philp@st-andrews.ac.uk
Fax: +44 (0)1334 463808; Tel: +44 (0)1334 467264.

ORCID IDs:
CCR: orcid.org/0000-0002-1419-9618
HWM: orcid.org/0000-0001-7575-2790
TK: orcid.org/0000-0001-7886-9660
DP: orcid.org/0000-0002-9198-4302

Abstract

A reciprocal replication system is constructed from four building blocks, **A**, **B**, **C**, and **D**, which react in a pairwise manner through either a 1,3-dipolar cycloaddition or the condensation reaction between an amine and an aldehyde to create two templates, *trans*-$\mathbf{T^{AB}}$ and $\mathbf{T^{CD}}$. These templates are equipped with complementary recognition sites—two carboxylic acids (*trans*-$\mathbf{T^{AB}}$) or two 4,6-dimethylamidopyridines ($\mathbf{T^{CD}}$)—that enable each template to direct the formation of its complementary partner through two mutually-reinforcing crosscatalytic pathways, in which the templates *trans*-$\mathbf{T^{AB}}$ or $\mathbf{T^{CD}}$ preorganize the appropriate building blocks within two catalytically-active ternary complexes: [**C**•**D**•*trans*-$\mathbf{T^{AB}}$] and [**A**•**B**•$\mathbf{T^{CD}}$]. The template-directed processes within these complexes generate a heteroduplex [*trans*-$\mathbf{T^{AB}}$•$\mathbf{T^{CD}}$], which is shown to possess significant stability through kinetic simulation and fitting. As a consequence, the individual crosscatalytic pathways perform more efficiently in template-directed experiments when the concentration of the template being formed is below that of the template added as instruction. Comprehensive analysis of the system when **A**, **B**, **C**, and **D** are mixed together directly, using a series of ^{1}H NMR spectroscopic kinetic experiments, demonstrates that the behavior of the reciprocal system is more than the simple sum of its parts—as part of the interconnected network, the product of each reaction clearly directs the fabrication of its reciprocal partner, facilitating both higher rates of formation for both templates and improved diastereoselectivity for *trans*-$\mathbf{T^{AB}}$. A simple change in experimental conditions (from dry to 'wet' $CDCl_3$) demonstrates the sensitivity of the replication pathways within the network to the reaction environment, which leads to a >10-fold increase in the contribution of a new minimal self-replicator, *trans*-$\mathbf{T^{AB*}}$, to the replication network.

Introduction

Networks constructed from individual components that interact and react with each other in pre-defined ways are a common feature at almost every length scale in the world around us—from the human immune system to patterns of weather in the atmosphere. The functions and behaviors expressed by these networks at a whole system level are derived from the interconnections[1] between their individual components. In the last 20 years, there has been significant growth in many disciplines[1,2] in the study of complexity and complex systems,[3] and the properties[4] that can emerge through the interactions of their constituent components. In chemistry, the nascent field[5] of systems chemistry has started to create synthetic chemical entities that can be assembled into complex networks that exhibit system-level behaviors[4a,b,g,5b,6] and functions by exploiting a bottom-up approach. Central to these strategies are the processes[7] that surround molecular replication. The auto- and crosscatalytic properties of synthetic replicators, coupled with their highly specific self- and mutual recognition properties, make them ideal building blocks from which to construct complex networks. Proponents of the systems chemistry approach have to date produced an array of replicating systems based on oligonucleotides,[8] peptides,[9] and small synthetic molecules.[10] These studies demonstrate clearly that replication is not the sole preserve of nucleic acids augmented by extensive enzymatic machinery. These replicators have been embedded within systems that can exhibit error-correction,[11] stereospecific replication,[12] Boolean logic,[13] as well as the capacity to respond to the reaction environment.[9g,h,j,10c,13d,14] The vast majority of synthetic replicators described to date rely on self-complementary templates, especially those based on simple organic compounds. In these so-called minimal replicating systems, a template that is complementary to itself directs its own formation through an autocatalytic cycle. It is, however, possible to construct a replicating system from two mutually complementary templates in which the catalytic effects are reciprocal. In such systems, each of the two non-identical, but mutually-complementary, templates directs the formation of its partner through two interlinked crosscatalytic cycles. The processes involved in reciprocal replication are encapsulated schematically in Figure 1.

The prototypical reciprocal replicating system (Figure 1) can be constructed from two sets of reagents, each bearing complementary recognition and reactive sites. In the system

shown in Figure 1, component **A** can react only with **B** and component **C** can react only with **D**. The bimolecular reactions of these two pairs of reagents create two templates, $\mathbf{T}^{AB}$ and $\mathbf{T}^{CD}$ (Figure 1). These templates do not have the necessary self-complementary recognition sites required for self-replication. Instead, the reciprocal nature of the non-covalent interactions between the two templates allows the $\mathbf{T}^{CD}$ template to crosscatalyze the formation of $\mathbf{T}^{AB}$ through the assembly of the catalytically-active ternary complex [**A**•**B**•$\mathbf{T}^{CD}$]. In the same manner, template $\mathbf{T}^{AB}$ is able to crosscatalyze the formation of $\mathbf{T}^{CD}$ through the assembly of the catalytically-active ternary complex [**C**•**D**•$\mathbf{T}^{AB}$].

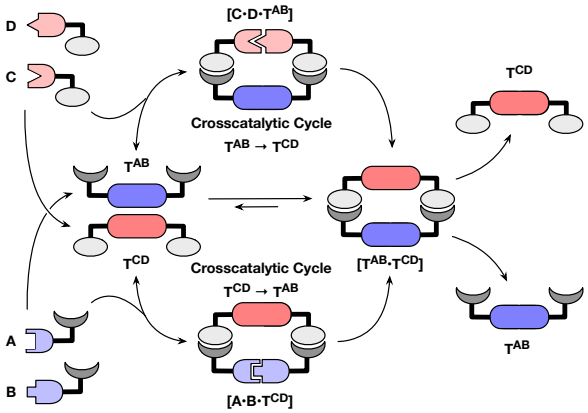

Figure 1 Two templates, $\mathbf{T}^{AB}$ and $\mathbf{T}^{CD}$, containing complementary recognition sites (light and dark gray) are formed initially through the bimolecular reactions between **A** and **B** (blue) and between **C** and **D** (red). Once formed, these templates can participate in two template-directed crosscatalytic cycles, where $\mathbf{T}^{AB}$ catalyzes the formation of $\mathbf{T}^{CD}$ through the assembly of **C** and **D** in a catalytically-active ternary complex [**C**•**D**•$\mathbf{T}^{AB}$], and *vice versa*. However, neither template $\mathbf{T}^{AB}$ nor $\mathbf{T}^{CD}$ possess the recognition sites required for self-replication. Taken together, these two crosscatalytic cycles ($\mathbf{T}^{AB} \rightarrow \mathbf{T}^{CD}$ and $\mathbf{T}^{CD} \rightarrow \mathbf{T}^{AB}$) represent a formal reciprocal replication cycle.

Ultimately, these processes afford the template heteroduplex [$\mathbf{T}^{AB}$•$\mathbf{T}^{CD}$] that can dissociate to return one molecule each of $\mathbf{T}^{AB}$ and $\mathbf{T}^{CD}$ back to the start of the respective catalytic cycles. These two interlinked cross-catalytic cycles represent a formal reciprocal replication cycle. It is important to note that the complexity of this system can increase dramatically depending on the nature of the chemical reactions employed to create the two templates from their constituents. In the case where the reaction between **A** and **B** and the reaction between **C** and **D** are chemically orthogonal, only the reciprocal replication cycle discussed above is present. However, if the system loses this chemical orthogonality and

reaction between, for example, **A** and **C** becomes possible, then additional minimal replication cycles can emerge through the formation of self-complementary templates.

Although several replicating networks involving oligonucleotides and peptides that participate in crosscatalytic interactions have been described previously,[8b,c,f,9a,d,h,11,14a] examples that are based on small, synthetic organic molecules are somewhat rare. Both the Rebek[15] laboratory and our own[16] have reported examples of systems that exhibit reciprocal template effects based on small organic molecules. However, in both these cases, a lack of orthogonality between the chemical ligation reactions used to construct the templates allowed the systems[15a,16a] to create selfish, autocatalytic templates and their presence diminished the overall importance of reciprocal replication in these systems. In order to create a purely reciprocal replicating system, unwanted reactivity between replicator components must be eliminated. In order to achieve this goal, we developed an orthogonal reactivity strategy for the creation of the two complementary templates shown in Figure 2.

Critical elements in replicator design are the recognition elements that drive the catalytic processes within the replication cycle. We have demonstrated previously[10a-c,e,f,13c,16,17] that hydrogen bonding between an amidopyridine and a carboxylic acid can be applied to direct autocatalytic processes. Accordingly, maleimide **A** and nitrone **B** are equipped with carboxylic acid recognition sites. Amine **C** and aldehyde **D** are equipped with complementary amidopyridine recognition sites, ensuring that templates $\mathbf{T^{AB}}$ and $\mathbf{T^{CD}}$ are mutually complementary. The association constant (K_a) for these recognition partners, determined[18] by ^{1}H NMR spectroscopic titration, is 3470 ± 300 M^{-1} in $CDCl_3$ at 283 K.

A key design element in our strategy is the use of the 1,3-dipolar cycloaddition between maleimide and nitrone (Figure 2). This reaction has been applied successfully in our laboratory[10a–c,e,13c,16,17a,b] to create several minimal replicating systems. Previously, we have also shown[19] that imine formation between an aniline and an aromatic aldehyde can proceed through a recognition-mediated pathway under conditions similar to those required for the 1,3-dipolar cycloaddition reaction. We therefore designed the system shown in Figure 2, in which we expected the reaction between maleimide **A** and nitrone **B**,

which forms $\mathbf{T}^{\mathbf{AB}}$, to be chemically orthogonal to the reaction between amine **C** and aldehyde **D**, which forms imine $\mathbf{T}^{\mathbf{CD}}$.

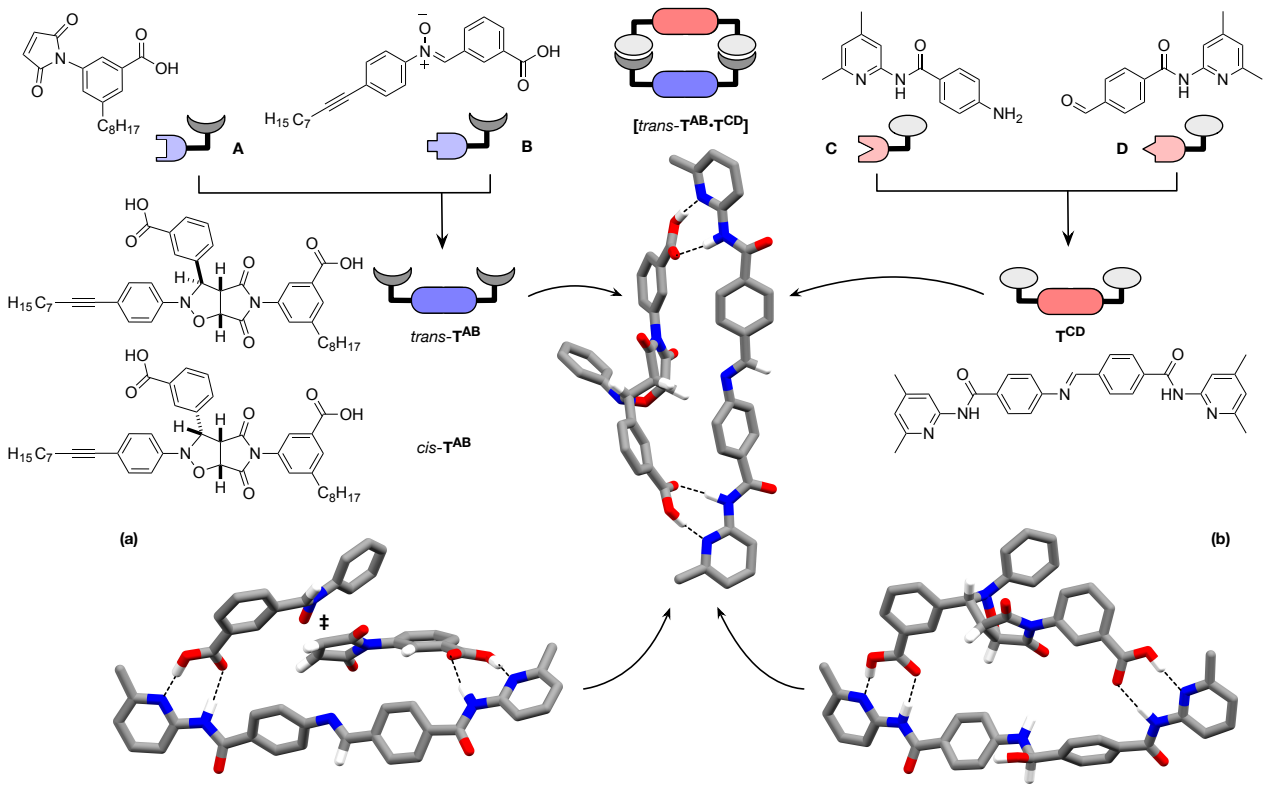

Figure 2 Four building blocks, **A**, **B**, **C**, and **D**, react in a pairwise manner to give two templates, *trans*-$\mathbf{T}^{\mathbf{AB}}$ and $\mathbf{T}^{\mathbf{CD}}$, which are equipped with mutually complementary recognition sites (carboxylic acid and 4,6-dimethylamidopyridien) that enable these templates to participate in two crosscatalytic pathways mediated by the formation of two catalytically active complexes: [**C**•**D**•*trans*-$\mathbf{T}^{\mathbf{AB}}$] and [**A**•**B**•$\mathbf{T}^{\mathbf{CD}}$]. Calculated structures of (a) the transition state (‡) accessed by [**A**•**B**•$\mathbf{T}^{\mathbf{CD}}$] and (b) the hemiaminal intermediate on the pathway to the corresponding template heteroduplex [*trans*-$\mathbf{T}^{\mathbf{AB}}$•$\mathbf{T}^{\mathbf{CD}}$]. Calculations performed at the ωB97X/def2-SVP level of theory using the polarized continuum solvation model for chloroform. Hydrogen bonds are represented using dashed blacked lines. Carbon atoms are colored gray, nitrogen atoms blue, oxygen atoms red, and hydrogen atoms white. Most hydrogen atoms are omitted for clarity.

The 1,3-dipolar cycloaddition reaction between **A** and **B** creates two diastereoisomeric products, *trans*-$\mathbf{T}^{\mathbf{AB}}$ and *cis*-$\mathbf{T}^{\mathbf{AB}}$. In order to understand the influence that template $\mathbf{T}^{\mathbf{CD}}$ might have on this process, we conducted a series of DFT calculations at the ωB97X/def2-SVP level of theory using a continuum solvation model for $CHCl_3$. These calculations reveal (Figure 2) that $\mathbf{T}^{\mathbf{CD}}$ is highly complementary to *trans*-$\mathbf{T}^{\mathbf{AB}}$. Further, the transition state leading to *trans*-$\mathbf{T}^{\mathbf{AB}}$ (Figure 2a) is accommodated on template $\mathbf{T}^{\mathbf{CD}}$ without significant distortion, suggesting that imine $\mathbf{T}^{\mathbf{CD}}$ should be capable of catalyzing the

formation of *trans*-$\mathbf{T^{AB}}$. By contrast, *cis*-$\mathbf{T^{AB}}$ possesses a folded structure that is not at all complementary with $\mathbf{T^{CD}}$. This observation suggests that $\mathbf{T^{CD}}$ would be incapable of catalyzing the formation of *cis*-$\mathbf{T^{AB}}$ and that the overall formation of $\mathbf{T^{AB}}$ should proceed diastereoselectively in the presence of $\mathbf{T^{CD}}$. Calculations also demonstrate that *trans*-$\mathbf{T^{AB}}$ is capable of accommodating the hemiaminal intermediate (Figure 2b), associated with the formation of imine $\mathbf{T^{CD}}$ without significant distortion, suggesting that *trans*-$\mathbf{T^{AB}}$ may also be capable of catalyzing the formation of imine $\mathbf{T^{CD}}$. Taken together, these results suggest that a reciprocal replication cycle can be established using *trans*-$\mathbf{T^{AB}}$ and $\mathbf{T^{CD}}$.

Results and discussion

In order to identify the presence of the crosscatalytic pathways and to assess their efficiencies, the pairwise reactions of maleimide **A** with nitrone **B** and aniline **C** with aldehyde **D** were examined first in isolation (*e.g.*, **A** and **B** were reacted in solution in the absence of either **C** and **D** or preformed template). Subsequently, the reactions of the two pairs of reagents were analyzed in the presence of the relevant reciprocal template (*e.g.*, reaction of **A** with **B** was examined in the presence of $\mathbf{T^{CD}}$ and *vice versa*). In each kinetic experiment, an equimolar solution of the required reagents (10 mM) was prepared in $CDCl_3$ and the appearance of products was monitored at regular intervals at 10 °C over 15 h by 500 MHz ^{1}H NMR spectroscopy. The concentrations of the products were determined by deconvolution of the resonances arising either from protons in the bicyclic ring system present in $\mathbf{T^{AB}}$ in the range δ 4.5 to 6.0 or the resonance arising from the imine proton in $\mathbf{T^{CD}}$ around δ 8.2 in comparison to appropriate resonances arising from the starting materials.

In isolation, the reaction between maleimide **A** and nitrone **B** (Figure 3a, filled circles) proceeds slowly and with limited diastereoselectivity, reaching an overall conversion of 23% after 15 h, with the concentrations of *trans*-$\mathbf{T^{AB}}$ and *cis*-$\mathbf{T^{AB}}$ reaching 1.74 mM and 0.58 mM, respectively ([*trans*-$\mathbf{T^{AB}}$]:[*cis*-$\mathbf{T^{AB}}$] = 3:1). Likewise, the reaction between aniline **C** and aldehyde **D** (Figure 3b, filled circles) afforded imine $\mathbf{T^{CD}}$, which reached a concentration of 0.68 mM after 15 h at 10 °C (7% conversion). Imine formation is a reversible process, and imine condensation is therefore expected to reach equilibrium after a certain time. After 14 days, the condensation between aniline **C** with aldehyde **D** had reached equilibrium at *ca.*

35% conversion to imine $\mathbf{T}^{CD}$. These results confirm that, in the absence of an appropriate reciprocal template, both *trans*-$\mathbf{T}^{AB}$ and $\mathbf{T}^{CD}$ are formed slowly, and, in the case of *trans*-$\mathbf{T}^{AB}$, with low diastereoselectivity.

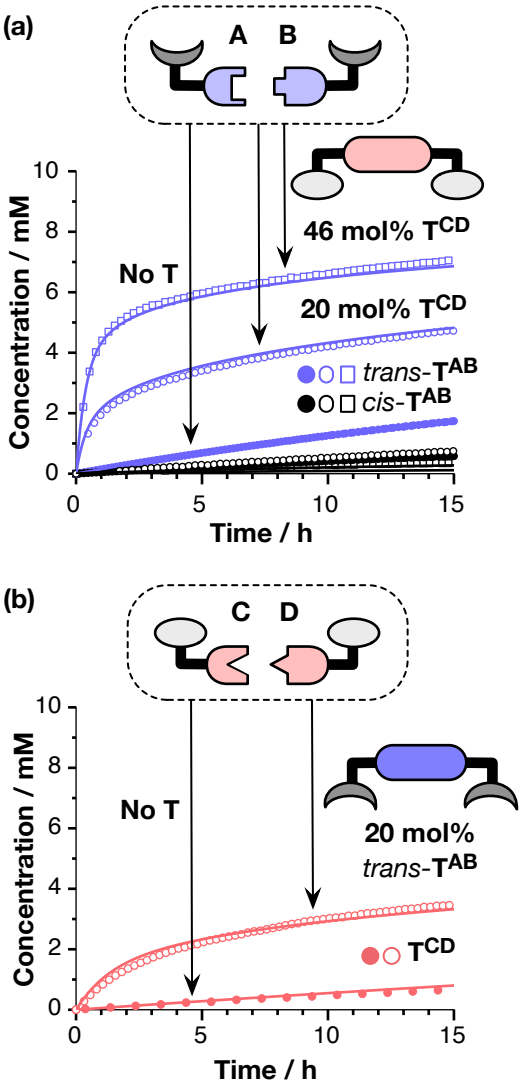

Figure 3 (a) Maleimide **A** reacts with nitrone **B** to give two diastereoisomeric products, *trans*-$\mathbf{T}^{AB}$ (blue) and *cis*-$\mathbf{T}^{AB}$ (black) in the absence of template (filled circles) and in the presence of 20 mol% (open circles) and 46 mol% (open squares) of preformed $\mathbf{T}^{CD}$. (b) Aniline **C** reacts with aldehyde **D** to give $\mathbf{T}^{CD}$ (red) in the absence of template (filled circles) and in the presence of 20 mol% of preformed *trans*-$\mathbf{T}^{AB}$ (open circles). The full lines represent the best fits of the appropriate kinetic models to the experimental data (see Supporting Information). Reaction conditions: [**A**] = [**B**] or [**C**] = [**D**] = 10 mM, 10 °C, $CDCl_3$. The reaction profiles were determined by deconvolution of 500 MHz ^{1}H NMR spectroscopic data; all concentrations have been corrected for the amount of template added.

In order to examine the capacity of imine $\mathbf{T^{CD}}$ to function as a template for the formation of *trans*-$\mathbf{T^{AB}}$, the reaction between maleimide **A** and nitrone **B** was repeated in the presence of 20 mol% of preformed $\mathbf{T^{CD}}$ added at t = 0 h. The concentration *vs.* time profile for this reaction (Figure 3a, open circles) is strikingly different to that for the uninstructed process. The production of *trans*-$\mathbf{T^{AB}}$ (open blue circles) is enhanced significantly. At t = 2 h, *trans*-$\mathbf{T^{AB}}$ reaches a concentration of 2.52 mM, *i.e.*, a value that exceeds the amount of *trans*-$\mathbf{T^{AB}}$ produced after 15 h in the absence of instruction by $\mathbf{T^{CD}}$. After 15 h, the concentrations of *trans*-$\mathbf{T^{AB}}$ and *cis*-$\mathbf{T^{AB}}$ had reached 4.72 mM and 0.75 mM, respectively, an overall conversion to both diastereoisomers of 55% ([*trans*-$\mathbf{T^{AB}}$]:[*cis*-$\mathbf{T^{AB}}$] = 6.3:1).

The reaction between maleimide **A** and nitrone **B** was also examined in the presence of 46 mol% of preformed $\mathbf{T^{CD}}$ added at t = 0 h. Again, the concentration *vs.* time profile for this reaction (Figure 3a, open squares) displays a significant enhancement in the formation of *trans*-$\mathbf{T^{AB}}$ when compared to the uninstructed process. The production of *trans*-$\mathbf{T^{AB}}$ (open blue squares) is enhanced significantly. At t = 2 h, *trans*-$\mathbf{T^{AB}}$ reaches a concentration of 5.19 mM, a value that exceeds the amount of *trans*-$\mathbf{T^{AB}}$ produced after 15 h in the presence of 20 mol% of $\mathbf{T^{CD}}$. After 15 h, the concentrations of *trans*-$\mathbf{T^{AB}}$ and *cis*-$\mathbf{T^{AB}}$ had reached 7.08 mM and 0.35 mM, respectively, an overall conversion to both diastereoisomers of 74% ([*trans*-$\mathbf{T^{AB}}$]:[*cis*-$\mathbf{T^{AB}}$] = 20.3:1). These results mirror the prediction from our DFT calculations, which suggested that $\mathbf{T^{CD}}$ should be an effective template for the formation of *trans*-$\mathbf{T^{AB}}$, resulting in an increase in the rate and diastereoselectivity for this reaction. By contrast, the conversion to *cis*-$\mathbf{T^{AB}}$ exhibited no significant change in the presence of $\mathbf{T^{CD}}$. Taken together, these observations verify our hypothesis that the imine $\mathbf{T^{CD}}$ can direct the formation of *trans*-$\mathbf{T^{AB}}$, but not *cis*-$\mathbf{T^{AB}}$.

In order to examine the efficiency of the second crosscatalytic pathway, the condensation reaction between aniline **C** and aldehyde **D** was performed in the presence of 20 mol% of preformed *trans*-$\mathbf{T^{AB}}$. The concentration–time profile for this reaction (Figure 3b, open circles) displayed an enhancement in the rate of formation of $\mathbf{T^{CD}}$. After 2 h, the concentration of imine $\mathbf{T^{CD}}$ reached 1.36 mM. Even at this early reaction time, the concentration of $\mathbf{T^{CD}}$ formed in this reaction exceeded that created in the absence of reciprocal template. After the initial period of *ca.* 3 h, the formation of $\mathbf{T^{CD}}$ proceeded at a

slower rate, reaching a concentration of 3.47 mM after 15 h, which represents an overall conversion of 35%. Clearly, the marked changes observed in the rate and extent of formation of imine $\mathbf{T^{CD}}$ in the presence of *trans*-$\mathbf{T^{AB}}$ confirm the efficiency of the second crosscatalytic pathway required for the establishment of the fully operational reciprocal system. Whilst it would be desirable to explore the effect of different concentrations of $\mathbf{T^{AB}}$ on the formation of $\mathbf{T^{CD}}$ more fully, unfortunately, the limited solubility of *trans*-$\mathbf{T^{AB}}$ in $CDCl_3$, arising from the presence of two carboxylic acids, precluded the examination of this crosscatalytic pathway at higher loadings of *trans*-$\mathbf{T^{AB}}$ template.

In order to quantify the changes observed in the two crosscatalytic pathways following the introduction of the reciprocal templates, we fitted the experimental data shown in Figure 3 to the appropriate kinetic models (for details, see the Supporting Information, Section S5). The data gave excellent fits (Figure 3, solid lines) to these models and allowed us to extract the key kinetic and thermodynamic parameters for the two control (uninstructed) and two template-directed pathways. Specifically, employing models that describe the key interactions and reactions leading to the formation of *trans*-$\mathbf{T^{AB}}$ and $\mathbf{T^{CD}}$, we were able to determine the bimolecular rate constants (k_{bi}) for the formation of *trans*-$\mathbf{T^{AB}}$ and *cis*-$\mathbf{T^{AB}}$, the unimolecular rate constant (k_{cat}) for the formation of *trans*-$\mathbf{T^{AB}}$ on $\mathbf{T^{CD}}$ template (*via* the ternary complex [$\mathbf{A \bullet B \bullet T^{CD}}$]) and the heteroduplex association constant ($K_a^{Heteroduplex}$) (Table 1). In addition, were able to determine the rates of the forward[20] reaction to give $\mathbf{T^{CD}}$, both in the absence and presence of *trans*-$\mathbf{T^{AB}}$ as instruction (Table 1). These parameters were used subsequently to calculate (Table 1) the kinetic[21,22] and thermodynamic[23] effective molarities ($EM_{kinetic}$ and EM_{thermo}, respectively) for the two template-directed crosscatalytic pathways.

Table 1 Overview of rate constants determined for the bimolecular and template-directed cycloaddition reaction and imine formation to give *trans*-$\mathbf{T^{AB}}$ and $\mathbf{T^{CD}}$, respectively. The heteroduplex association constant ($K_a^{Heteroduplex}$) was estimated to be 3.35×10^7 M^{-1}. The k_{bi} for the formation of *cis*-$\mathbf{T^{AB}}$ was determined to be 1.40×10^{-4} M^{-1} s^{-1}.

	Cycloaddition Reaction	***k***	**$EM_{kinetic}$ / M**
Bimolecular k_{bi} / 10^{-4} M^{-1} s^{-1}	**A** + **B** → *trans*-$\mathbf{T^{AB}}$	4.20 ± 0.01	—
Template-directed k_{cat} / 10^{-4} s^{-1}	[**A**•**B**•$\mathbf{T^{CD}}$] → [*trans*-$\mathbf{T^{AB}}$•$\mathbf{T^{CD}}$]	21.1 ± 0.02	5.02

	Imine Formation	***k***	**$EM_{kinetic}$ / M**
Bimolecular k_{bi} / 10^{-4} M^{-1} s^{-1}	**C** + **D** → $\mathbf{T^{CD}}$	1.61 ± 0.00	—
Template-directed k_{cat} / 10^{-4} s^{-1}	[**C**•**D**•*trans*-$\mathbf{T^{AB}}$] → [*trans*-$\mathbf{T^{AB}}$•$\mathbf{T^{CD}}$]	5.55 ± 0.002	3.44

Examination of the parameters summarized in Table 1 reveals that, in the presence $\mathbf{T^{CD}}$, the formation of *trans*-$\mathbf{T^{AB}}$ is associated with an $EM_{kinetic}$ of 5.02 M, whereas, the formation of $\mathbf{T^{CD}}$ (*via* the key catalytically-active complex [**C**•**D**•*trans*-$\mathbf{T^{AB}}$]) is associated with an $EM_{kinetic}$ of 3.44 M. These results demonstrate that the mutually complementary templates *trans*-$\mathbf{T^{AB}}$ and $\mathbf{T^{CD}}$ are capable of accelerating the formation of each other efficiently *via* the two crosscatalytic template-directed pathways.

A key element in this system is the heteroduplex [*trans*-$\mathbf{T^{AB}}$•$\mathbf{T^{CD}}$] (Figure 2)—the stability of this duplex controls the availability of the catalytically-active templates in solution. This duplex is expected to be very stable and an assessment of its stability was not possible directly[24] using ^{1}H NMR spectroscopic methods. From our kinetic simulation and fitting, we were able to confirm that the [*trans*-$\mathbf{T^{AB}}$•$\mathbf{T^{CD}}$] complex is, indeed, very stable, having an association constant ($K_a^{Heteroduplex}$) that is in excess 10^7 M^{-1}. This association constant corresponds to a connection EM[25] (EM_{thermo}) of 2.8 M indicating that there is a high level of complementarity between these two templates. The direct consequence of the stable [*trans*-$\mathbf{T^{AB}}$•$\mathbf{T^{CD}}$] complex is the apparent biphasic character of the kinetic profiles for the template-directed experiments shown in Figure 3 (blue and red open symbols). For example, when the formation of *trans*-$\mathbf{T^{AB}}$ is being instructed by $\mathbf{T^{CD}}$, as long as the concentration of *trans*-$\mathbf{T^{AB}}$ is below that of $\mathbf{T^{CD}}$ added initially, there must always be unbound $\mathbf{T^{CD}}$ available to accelerate the formation of *trans*-$\mathbf{T^{AB}}$. This situation arises as a result of the maximum concentration of the tightly bound complex [*trans*-$\mathbf{T^{AB}}$•$\mathbf{T^{CD}}$] being determined by the concentration of *trans*-$\mathbf{T^{AB}}$ formed. However, once the concentration of *trans*-$\mathbf{T^{AB}}$ exceeds

that of $\mathbf{T}^{\mathbf{CD}}$, the efficiency of the system is reduced dramatically as the stability of the [*trans*-$\mathbf{T}^{\mathbf{AB}}\bullet\mathbf{T}^{\mathbf{CD}}$] heteroduplex now controls the availability of free $\mathbf{T}^{\mathbf{CD}}$ in solution. This effect can be seen clearly in the data shown in Figure 3a—the change in reaction rate occurs at [*trans*-$\mathbf{T}^{\mathbf{AB}}$] = 2 mM when 20 mol% of $\mathbf{T}^{\mathbf{CD}}$ is added and at about 4.5 mM when 46 mol% of $\mathbf{T}^{\mathbf{CD}}$ is added. An identical argument can be constructed for the reverse catalytic situation where $\mathbf{T}^{\mathbf{CD}}$ is constructed on *trans*-$\mathbf{T}^{\mathbf{AB}}$.

Having characterized the individual pathways present in the reciprocal system, we next set out to combine the four starting materials within a single experiment. In this situation, we envisaged that the *in situ* formation of *trans*-$\mathbf{T}^{\mathbf{AB}}$ would catalyze the formation of imine $\mathbf{T}^{\mathbf{CD}}$ and *vice versa*, allowing the formation of a reciprocal, mutually reinforcing replicating system. To this end, an equimolar mixture (10 mM) of **A**, **B**, **C**, and **D** was prepared in $CDCl_3$ and the formation of $\mathbf{T}^{\mathbf{AB}}$ and $\mathbf{T}^{\mathbf{CD}}$ (Figure 4a) was monitored at 10 °C over 40 h using 500 MHz ^{1}H NMR spectroscopy.

Examination of the concentration-time profiles of the products formed from the four-component system (Figure 4a) reveals that the major products are the two reciprocal templates *trans*-$\mathbf{T}^{\mathbf{AB}}$ and $\mathbf{T}^{\mathbf{CD}}$. The data reveals the presence of a small initial lag period for the formation of *trans*-$\mathbf{T}^{\mathbf{AB}}$ and a more pronounced initial lag period in the formation of $\mathbf{T}^{\mathbf{CD}}$. The presence of the sigmoidal concentration-time profiles for both templates is directly related to the processes and reactions inherent (Figure 1) in mutually crosscatalytic reciprocal replication. Specifically, at the start of the reaction, the reciprocal templates can only be formed through the uncatalyzed bimolecular pathways. The rates at which *trans*-$\mathbf{T}^{\mathbf{AB}}$ and $\mathbf{T}^{\mathbf{CD}}$ are formed start to increase once the template-mediated processes begin to operate efficiently, *i.e.*, when the concentration of each template exceeds the value of K_d for the binding of the building blocks, **A**, **B**, **C**, and **D**, to the appropriate template, forming the catalytically-active ternary complexes. Finally, the depletion of the starting materials eventually leads to a decrease in the rates at which the two reciprocal templates are produced.

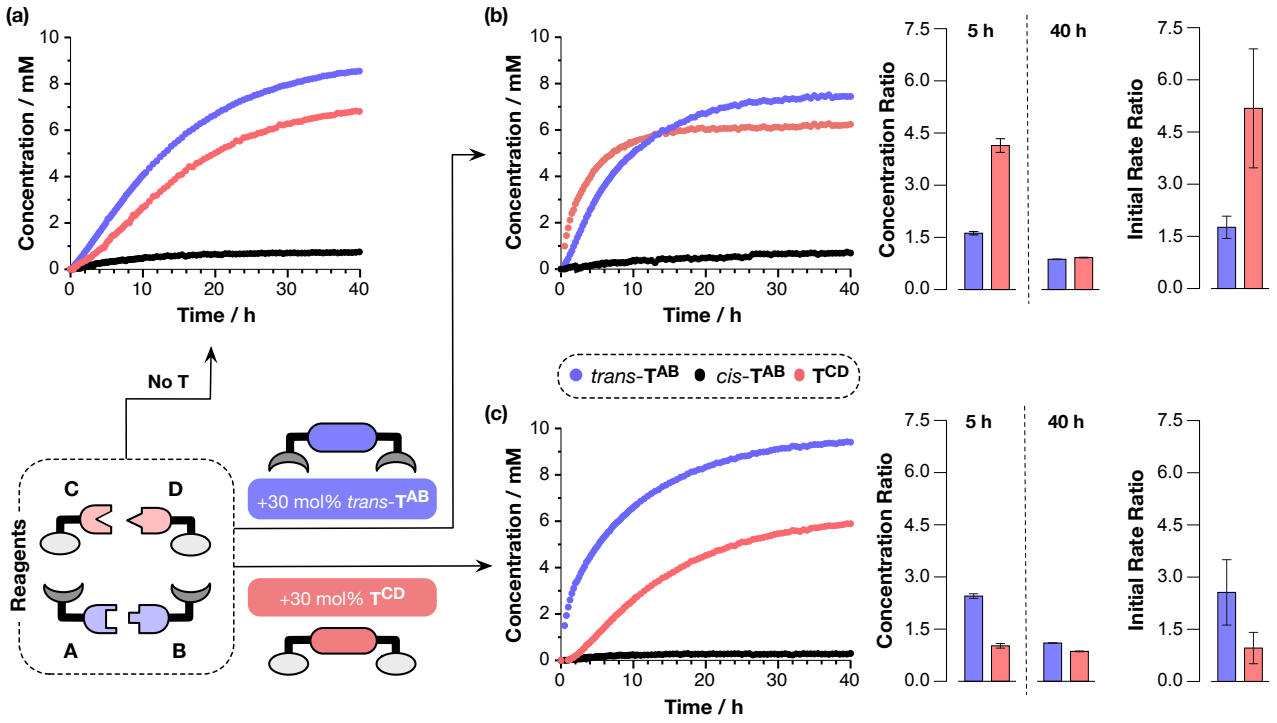

$$\text{Concentration Ratio} = \frac{[\text{T}]_t \text{ (Instructed)}}{[\text{T}]_t \text{ (Uninstructed)}} \qquad \text{Initial Rate Ratio} = \frac{\text{Rate}_{initial} \text{ (Instructed)}}{\text{Rate}_{initial} \text{ (Uninstructed)}}$$

Figure 4 A reciprocal replication network is constructed by the reaction of maleimide **A**, nitrone **B**, aniline **C**, and aldehyde **D** to give two diastereoisomeric products, *trans*-**T**^{AB} (blue) and *cis*-**T**^{AB} (black), and imine **T**^{CD} (red) (a) in the absence of any added template as instruction, and in the presence of (b) 30 mol% of preformed *trans*-**T**^{AB}, or (c) 30 mol% of preformed **T**^{CD}. The impact of the added template on the formation of *trans*-**T**^{AB} and **T**^{CD} is demonstrated by comparison of the concentration ratios calculated at t = 5 h and 40 h, and the ratios of initial rates for the formation of the templates. Reaction conditions: [**A**] = [**B**] = [**C**] = [**D**] = 10 mM, 10 °C, $CDCl_3$. The reaction profiles were determined by deconvolution of 500 MHz ^{1}H NMR spectroscopic data; all concentrations have been corrected for the amount of template added. A description of the error analysis is provided in the Supporting Information.

Comparison of this experiment with the uninstructed formation of *trans*-**T**^{AB} or **T**^{CD} in isolation (data in Figure 3, filled circles) reveals striking differences in behavior. In the case of *trans*-**T**^{AB}, the overall conversion to this product in the four-component system after 5 h (Figure 4a) was 20%, with the diastereoselectivity being 6.3:1 in favor of *trans*-**T**^{AB}. These values can be compared with those from the data in Figure 3a at t = 5 h— conversion = 7% and a diastereoselectivity of only 3:1 in favor of *trans*-**T**^{AB}. Similarly, the condensation of **C** and **D** to form imine **T**^{CD} was also enhanced within the four-component system—the conversion of **C** and **D** to **T**^{CD} reached 11% after 5 h (Figure 4a) in comparison to <3% in the data shown in Figure 3b after the same time. These results demonstrate the mutually-reinforcing effect of the two crosscatalytic cycles when they operate together within a shared

environment and these template-directed replication processes enhance both the rates of formation of *trans*-$\mathbf{T^{AB}}$ and $\mathbf{T^{CD}}$ and the diastereoselectivity for the formation of *trans*-$\mathbf{T^{AB}}$. This situation is in direct contrast to the conditions used to acquire the data presented in Figure 3. In these experiments, the concentration of the instructing template remains constant throughout the entire duration of the experiment, since only two out of the four possible building blocks are present at a time. By contrast, the data in Figure 4 relates to experiments where all four building blocks are present and, consequently, the concentrations of the instructing templates are variable across the time course of the experiments. Thus, the comparison between the data shown in Figure 3 and Figure 4 must be limited to a qualitative assessment evidencing the nature of the mutually reinforcing nature of the reciprocal relationship between replicators $\mathbf{T^{AB}}$ and $\mathbf{T^{CD}}$.

In order to demonstrate the importance of template effects in this reciprocal replication system, two template-instructed experiments were performed. Firstly, the four reagents **A** to **D** were reacted at starting concentrations of 10 mM in $CDCl_3$ at 10 °C in the presence of 30 mol% of preformed *trans*-$\mathbf{T^{AB}}$ added at t = 0 h. These data (Figure 4b) show a rapid increase in the concentration of imine $\mathbf{T^{CD}}$, the initial rate of formation of $\mathbf{T^{CD}}$ is 1.01 mM h^{-1} (compared to 0.20 mM h^{-1} in the absence of template), with the concentration of $\mathbf{T^{CD}}$ reaching 4.48 mM after 5 h. After this point, the rate of formation of $\mathbf{T^{CD}}$ slows significantly and the concentration of $\mathbf{T^{CD}}$ only increases a further 1.76 mM to 6.24 mM at the end of the experiment after 40 h. In order to make comparisons with the uninstructed data, we calculated the ratios of template concentrations (at 5 h and 40 h) and initial rates, as shown in Figure 4. These ratios will take values that are >1 when enhancement occurs in the template-instructed experiment and values <1 when reduction in a given parameter is observed. Comparing the data in Figure 4b with that obtained under the same conditions in the absence of added *trans*-$\mathbf{T^{AB}}$ (Figure 4a) reveals some significant differences. The initial rate ratio for the formation of $\mathbf{T^{CD}}$ in the presence of *trans*-$\mathbf{T^{AB}}$ is 5.18, and the concentration ratio for $\mathbf{T^{CD}}$ after 5 h is 4.14. By contrast, at 40 h, the concentration ratio for $\mathbf{T^{CD}}$ is 0.92. These observations indicate that the most significant effects arising from the addition of template are present at early reaction times. This result is entirely consistent with the behavior observed in the experiments where $\mathbf{T^{CD}}$ is formed in isolation (data in Figure 3b). Once the

concentration of $\mathbf{T}^{\mathbf{CD}}$ becomes comparable to that of the instructing template, product inhibition resulting from the extremely stable [*trans*-$\mathbf{T}^{\mathbf{AB}}$•$\mathbf{T}^{\mathbf{CD}}$] duplex becomes progressively dominant in the system. As *trans*-$\mathbf{T}^{\mathbf{AB}}$ does not catalyze directly its own formation, it may seem counterintuitive to expect that the addition of *trans*-$\mathbf{T}^{\mathbf{AB}}$ to the system will affect the rate and extent of formation of itself. Nevertheless, this experiment reveals that the addition of *trans*-$\mathbf{T}^{\mathbf{AB}}$ does indeed have an effect on the rate of its own formation as a result of the reciprocal nature of the entire system. The initial rate of formation of *trans*-$\mathbf{T}^{\mathbf{AB}}$ = 0.71 mM h^{-1} (compared to 0.40 mM h^{-1} in the absence of template), with the concentration of *trans*-$\mathbf{T}^{\mathbf{AB}}$ reaching 3.25 mM after 5 h. Once again after this point, the rate of formation of *trans*-$\mathbf{T}^{\mathbf{AB}}$ slows and the concentration of *trans*-$\mathbf{T}^{\mathbf{AB}}$ increases a further 4.20 mM to 7.45 mM at the end of the experiment after 40 h. Despite the fact that *trans*-$\mathbf{T}^{\mathbf{AB}}$ does not template its own formation, the increase in the rate of production of $\mathbf{T}^{\mathbf{CD}}$, engendered by the addition of *trans*-$\mathbf{T}^{\mathbf{AB}}$ as an instruction, results in an initial rate ratio for the formation of *trans*-$\mathbf{T}^{\mathbf{AB}}$ of 1.76 by virtue of its crosscatalytic connection to $\mathbf{T}^{\mathbf{CD}}$. This enhancement in the rate of formation of *trans*-$\mathbf{T}^{\mathbf{AB}}$ also results in a dramatic increase in the diastereoselectivity for the formation of *trans*-$\mathbf{T}^{\mathbf{AB}}$ after 5 h to 19.3:1. The enhancement in the formation of $\mathbf{T}^{\mathbf{AB}}$ in the presence of $\mathbf{T}^{\mathbf{CD}}$ was also evidenced by the significant changes in the concentration *vs.* time profile of $\mathbf{T}^{\mathbf{AB}}$ observed in the presence of preformed $\mathbf{T}^{\mathbf{AB}}$ (Figure 4b) when compared to the uninstructed scenario (Figure 4a). These changes arise as a result of the efficient crosscatalytic formation of $\mathbf{T}^{\mathbf{AB}}$ on $\mathbf{T}^{\mathbf{CD}}$—our kinetic analyses demonstrate that $\mathbf{T}^{\mathbf{CD}}$ is a much better catalyst for the formation of $\mathbf{T}^{\mathbf{AB}}$ (k_{cat} = 21.1 × 10^{-4} s^{-1}) than $\mathbf{T}^{\mathbf{AB}}$ is for the formation of $\mathbf{T}^{\mathbf{CD}}$ (k_{cat} = 5.55 × 10^{-4} s^{-1}).

Secondly, the four reagents **A** to **D** were reacted at starting concentrations of 10 mM in $CDCl_3$ at 10 °C in the presence of 30 mol% of preformed $\mathbf{T}^{\mathbf{CD}}$ added at t = 0 h. These data (Figure 4c) show a rapid increase in the concentration of *trans*-$\mathbf{T}^{\mathbf{AB}}$, and the initial rate of formation of *trans*-$\mathbf{T}^{\mathbf{AB}}$ is 1.02 mM h^{-1}, with the concentration of *trans*-$\mathbf{T}^{\mathbf{AB}}$ reaching 4.91 mM after 5 h. After this point, the rate of formation of *trans*-$\mathbf{T}^{\mathbf{AB}}$ slows and the concentration of this template increases a further 4.50 mM to 9.41 mM at the end of the experiment after 40 h. Comparing the data in Figure 4c with that obtained under the same conditions in the absence of any preformed template (Figure 4a) once again reveals some significant

differences. The ratio of initial rates for the formation of *trans*-$\mathbf{T^{AB}}$ is 2.56 and the concentration ratio calculated for *trans*-$\mathbf{T^{AB}}$ is 2.45 after 5 h. Once again, this enhancement in the rate of formation of *trans*-$\mathbf{T^{AB}}$ also manifests in a dramatic increase in the diastereoselectivity for the formation of *trans*-$\mathbf{T^{AB}}$ after 5 h to 29:1. By contrast, at 40 h, the concentration ratio for *trans*-$\mathbf{T^{AB}}$ has a value of 1.10, although the diastereoselectivity for the formation of *trans*-$\mathbf{T^{AB}}$ remains high, at 32:1. These observations once again indicate that the most significant effects arising from the addition of the preformed template are most significant at early reaction times. This result is again consistent with the behavior observed in the experiments where *trans*-$\mathbf{T^{AB}}$ is formed in isolation (data in Figure 3a)—once the concentration of *trans*-$\mathbf{T^{AB}}$ becomes comparable to that of the instructing template added initially, product inhibition arising from the extremely stable [*trans*-$\mathbf{T^{AB}}$•$\mathbf{T^{CD}}$] duplex becomes progressively dominant in the system. In contrast to the previous experiment, $\mathbf{T^{CD}}$ does not benefit from either an enhancement in initial rate or, indeed, extent of its formation in the same manner as *trans*-$\mathbf{T^{AB}}$ when it was used as the instructing template. The concentration ratios calculated for $\mathbf{T^{CD}}$ at both 5 h and 40 h are close to one (1.02 and 0.86, respectively). The same trend is observed for the initial rate ratio for $\mathbf{T^{CD}}$, which is found to be 0.96. This observation can be rationalized by the fact that formation of $\mathbf{T^{CD}}$ is a dynamic process and the total concentration of $\mathbf{T^{CD}}$ that can be achieved is subject to a global equilibrium condition for the system. As we have added $\mathbf{T^{CD}}$ to this reaction at an initial concentration of 3 mM, the reaction starts at a point that is inherently closer to this global equilibrium position for the formation of $\mathbf{T^{CD}}$. As a consequence, we would expect the formation of $\mathbf{T^{CD}}$ to behave differently in this situation compared to the other two experiments in which the initial concentration of $\mathbf{T^{CD}}$ is zero.

It is clear from these results that the behavior of the reciprocal system is more than the simple sum of its parts. In the absence of a reciprocal template, each of the reactions proceeds slowly, and in the case of the cycloaddition, also with poor diastereoselectivity. As part of an interconnected network, however, the product of each reaction is clearly capable of facilitating the fabrication of its reciprocal partner, facilitating both higher reaction rates and diastereoselectivity.

The effect of reaction environment on the reciprocal replicators

The kinetic experiments described thus far confirm conclusively that the two reciprocal templates, *trans*-$\mathbf{T^{AB}}$ and $\mathbf{T^{CD}}$, are the dominant products that emerge from a reagent pool that contains **A**, **B**, **C** and **D**. However, under appropriate conditions, nitrone **B**, which is used in the creation of *trans*-$\mathbf{T^{AB}}$, is susceptible to hydrolysis. Under hydrolytic conditions, this nitrone affords aldehyde **1** and hydroxylamine **2** (Figure 5a) and, in this situation, hydroxylamine **2** can react with aldehyde **D** to afford a new nitrone **B***, which is equipped with an amidopyridine recognition site. Nitrone **B*** can then react in a 1,3-dipolar cycloaddition reaction with maleimide **A** to form cycloadduct *trans*-$\mathbf{T^{AB*}}$. However, in contrast to *trans*-$\mathbf{T^{AB}}$, which can, by virtue of its two identical recognition sites, act only as a catalyst for the formation of $\mathbf{T^{CD}}$, *trans*-$\mathbf{T^{AB*}}$ possesses recognition sites that render this template self-complementary. As a consequence, *trans*-$\mathbf{T^{AB*}}$ is capable[26] of directing its own formation through an autocatalytic template-directed pathway (Figure 5b). This possibility gives rise to an interesting scenario in which the environment in which the replicators derived from **A**, **B**, **C**, and **D** operate can promote either the reciprocal replication cycle mediated by *trans*-$\mathbf{T^{AB}}$ and $\mathbf{T^{CD}}$, or, alternatively, a minimal replication pathway mediated by *trans*-$\mathbf{T^{AB*}}$, or, indeed, a mixture of both of these pathways. Thus far, the environmental conditions were selected specifically to avoid hydrolysis and thereby ensure that the reciprocal replication cycle is dominant.

Under these conditions, the ratio of the reciprocal template *trans*-$\mathbf{T^{AB}}$ to the minimal replicator template *trans*-$\mathbf{T^{AB*}}$ was 49:1. If the rate of hydrolysis of nitrone **B** is enhanced in the four-component reaction, we would expect to observe an increase in the concentration of the amidopyridine-bearing nitrone **B***. In turn, the contribution of minimal replication, mediated by the template *trans*-$\mathbf{T^{AB*}}$, should also increase relative to the reciprocal replication cycle involving *trans*-$\mathbf{T^{AB}}$ and $\mathbf{T^{CD}}$.

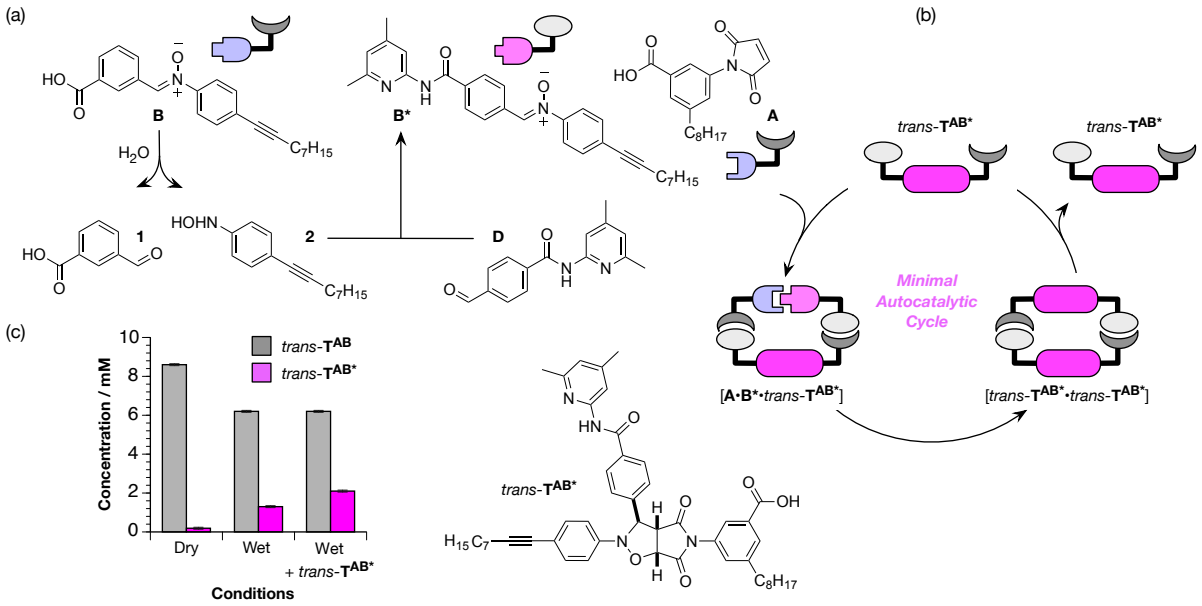

Figure 5 (a) In wet $CDCl_3$, nitrone **B** can hydrolyze to afford aldehyde **1** and hydroxylamine **2**. When these conditions are employed for the reaction of **A**, **B**, **C**, and **D**, hydroxylamine **2** can react with aldehyde **D** to afford nitrone **B***, bearing the 4,6-dimethylamidopyridine recognition site. (b) Reaction of nitrone **B*** with maleimide **A** produces *trans*-$\mathbf{T}^{\mathbf{AB*}}$ (magenta), which is capable of directing its own formation by the assembly of **A** and **B*** into a catalytically-active ternary complex [**A**•**B***•*trans*-$\mathbf{T}^{\mathbf{AB*}}$]. (c) Under dry conditions, reagents **A** to **D** react to produce the reciprocal replicator *trans*-$\mathbf{T}^{\mathbf{AB}}$ and minimal self-replicator *trans*-$\mathbf{T}^{\mathbf{AB*}}$ in a ratio of 49:1. Under wet conditions, the ratio of [*trans*-$\mathbf{T}^{\mathbf{AB}}$]:[*trans*-$\mathbf{T}^{\mathbf{AB*}}$] decreases markedly to 5:1, and the addition of preformed *trans*-$\mathbf{T}^{\mathbf{AB*}}$ decreases this ratio even further to 3:1. All concentrations have been corrected for the amount of template added. A description of the error analysis is provided in the Supporting Information.

In order to create the environmental conditions necessary to promote nitrone hydrolysis, we saturated $CDCl_3$ with water[27] to create conditions that were suitably 'wet'. Specifically, $CDCl_3$ was stirred for 20 min with D_2O before the aqueous and the organic layers were allowed to separate. Recovery of the organic layer afforded a sample of $CDCl_3$ in which the concentration of D_2O was >1500 ppm, as determined by Karl–Fisher titration. This sample of $CDCl_3$ was used to prepare a four-component experiment in which **A**, **B**, **C**, and **D** (each at a starting concentration of 10 mM) were allowed to react with each other for 40 h at 10 °C. Analysis of this experiment after this time by 500 MHz ^{1}H NMR spectroscopy revealed that the concentration of *trans*-$\mathbf{T}^{\mathbf{AB}}$ had decreased from 8.6 mM to 6.2 mM, while the concentration of *trans*-$\mathbf{T}^{\mathbf{AB*}}$ had increased from <200 μM to 1.3 mM (Figure 5c). Under these 'wet' conditions, therefore, the reciprocal and minimal templates *trans*-$\mathbf{T}^{\mathbf{AB}}$ and *trans*-$\mathbf{T}^{\mathbf{AB*}}$ were present in a ratio of 5:1—representing a 10-fold increase in the contribution of the minimal replicator to replication in this system, a dramatic change induced by a simple

change in the environmental conditions. It is well established that minimal replication pathways can be promoted by the addition of an autocatalytic template at the start of the reaction. Accordingly, we performed an experiment in which 20 mol% of preformed *trans*-$\mathbf{T}^{\mathbf{AB*}}$ was added to a mixture of the four building blocks, **A** to **D**, at 10 mM in 'wet' $CDCl_3$. The presence of *trans*-$\mathbf{T}^{\mathbf{AB*}}$ in this experiment engendered a further enhancement in the quantity of the minimal self-replicator formed and *trans*-$\mathbf{T}^{\mathbf{AB*}}$ reached a concentration of 2.1 mM after 40 h—representing a 3:1 ratio of the reciprocal template *trans*-$\mathbf{T}^{\mathbf{AB}}$ to the minimal template *trans*-$\mathbf{T}^{\mathbf{AB*}}$.

Although the reciprocal template *trans*-$\mathbf{T}^{\mathbf{AB}}$ remained as the dominant species in the system, even in the presence of added preformed *trans*-$\mathbf{T}^{\mathbf{AB*}}$, the marked increase in the contribution of the minimal self-replication pathway demonstrates the considerable power of both template instruction and environmental conditions in determining the outcome of replication processes. It can be envisaged that a similar reciprocal system constructed from building blocks that are more susceptible to hydrolysis would permit the construction of a replication system in which a change in the reaction environment could be used to steer the system towards either reciprocal or minimal replication pathways with increased selectivity. Such changes can be further complemented by changes in other environmental parameters such light, temperature, or pH, which can alter[9g,h,j,13d,14b] the efficiencies of the replication pathways and even turn them on[28] and off.

Conclusions

In conclusion, we have designed and implemented a reciprocal replication network that is constructed from a pair of mutually-complementary templates that are based on simple, synthetic organic molecules. The formation of this pair of complementary templates is driven by orthogonal 1,3-dipolar cycloaddition and imine condensation reactions. The formation of each template is accelerated markedly in the presence of its reciprocal partner. The fully functional replicating network can be established and maintained simply by mixing the four reagents required to synthesize the two templates in a single flask. In this situation, the mutually reinforcing nature of the exclusively reciprocal replicating system enhances the formation of both templates well above the levels observed when these

templates are examined in isolation. The reciprocal replication network also responds to the introduction of instructional templates. When either of the two templates are added to the reaction mixture containing all four reagents, the network responds to this instruction by enhancing the formation of both its reciprocal partner and the instructional template itself by virtue of the symbiotic nature of the reciprocal catalytic relationships within the network. The creation of this reciprocal replicating system opens the way for the implementation of the complex functions[29] provided by networks constructed from oligonucleotides and peptides using simple, synthetic organic molecules. Critical to the success of the reciprocal replicating system reported here is the orthogonality of the reactions that form the two templates. We envisage applying this technology to the creation of responsive networks in which the replication pathways can be controlled by template inputs as well as environmental factors, such as pH or water content.

Acknowledgements

The financial support for this work was provided by EaStCHEM and the Engineering and Physical Sciences Research Council (Grant EP/K503162/1). The authors acknowledge the contributions of Eleftherios Kassianidis, Evan Wood and Thomas Smith to early, exploratory work in this area.

Competing financial interests

The authors declare no competing financial interests.

Supporting Information

The Supporting information is available free of charge on the ACS Publications website:
General experimental procedures; synthetic procedures and compound characterization; details of kinetic analyses, fitting (including scripts), error determination, and details of DFT calculations.

Author Information

Corresponding author

* d.philp@st-andrews.ac.uk; Fax: +44 (0)1334 463808; Tel: +44 (0)1334 467264.

Present Addresses

‡ Department of Chemistry, University of Sheffield, Brook Hill, Sheffield S3 7HF, United Kingdom

† Institute of Structural and Molecular Biology, Division of Biosciences, University College London, Darwin Building, Gower Street, London WC1E 6BT, United Kingdom

Notes and References

(1) (a) Newmann, M. E. J. *SIAM Rev.* **2003**, *45*, 167. (b) Barabaśi, A.-L. *Rev. Mod. Phys.* **2002**, *74*, 1. (c) Strogatz, S. H. *Nature* **2001**, *410*, 268.

(2) (a) Mitchell, M. *Complexity: A Guided Tour*; Oxford University Press: New York, 2009. (b) Watts, D. J. *Small Worlds: The Dynamics of Networks between Order and Randomness*; Princeton University Press: NJ, 2003. (c) Barabaśi, A.-L. *Linked: The New Science of Networks*; Perseus Book Group: New York, 2002.

(3) (a) Holovatch, Y.; Kenna, R.; Thurner, S. *Eur. J. Phys.* **2017**, *38*, 023002. (b) Ladyman, J.; Lambert, J.; Wiesner, K. *Eur. J. Phil. Sci.* **2013**, *3*, 33. (c) Barabási, A.-L.; Oltvai, Z. N. *Nature Rev. Genet.* **2004**, *5*, 101. (d) Goldenfeld, N.; Kadanoff, L. P. *Science* **1999**, *284*, 87. (e) Kauffman, S. A. *At Home in the Universe: The Search for the Laws of Self-Organization and Complexity*; Oxford University Press Inc.: New York, 1995.

(4) (a) Armao IV, J. J.; Lehn, J.-M. *Angew. Chem., Int. Ed.* **2016**, *55*, 13450. (b) Semenov, S. N.; Kraft, L. J.; Ainla, A.; Zhao, M.; Baghbanzedeh, M.; Campbell, V. E.; Kang, K.; Fox, J. M.; Whitesides, G. M. *Nature* **2016**, *537*, 656. (c) Lehn, J.-M. *Proc. Natl. Acad. Sci. U. S. A.* **2002**, *99*, 4763. (d) Arthur, W. B. *Science* **1999**, *284*, 107. (e) Rind, D. *Science* **1999**, *284*, 105. (f) Weng, G.; Bhalla, U. S.; Iyengar, R. *Science* **1999**, *284*, 92. (g) Whitesides, G. M.; Ismagilov, R. F. *Science* **1999**, *284*, 89.

(5) (a) *The Emergence of Systems Chemistry*, Kisakürek, M. V. Ed.; Natural and Life Sciences Publishers: Switzerland, 2018. (b) Ashkenasy, G.; Hermans, T. M.; Otto, S.; Taylor, A. F.; *Chem. Soc. Rev.* **2017**, *46*, 2543. (c) Islam, S.; Powner, M. W. *Chem.* **2017**, *2*, 470. (d) de la Escosura, A.; Briones, C.; Ruiz- Mirazo, K. *J. Theor. Biol.* **2015**, *381*, 11. (e) Mattia, E.; Otto, S. *Nat. Nanotechnol.* **2015**, *10*, 111. (f) Ruiz-Mirazo, K.; Briones, C.; de la Escosura, A. *Chem. Rev.* **2014**, *114*, 285. (g) Nitschke, J. R. *Nature* **2009**, *462*, 736. (h) Stankiewicz, J.; Eckardt, L. H. *Angew. Chem., Int. Ed.* **2006**, *45*, 342.

(6) (a) Taylor, J. W.; Eghtesadi, S. A.; Points, L. J.; Cronin, L. *Nat. Commun.* **2017**, *8*, 237. (b) Wong, A. S. Y.; Pogodaev, A. A.; Vialshin, I. N.; Helwig, B.; Huck, W. T. S. *J. Am. Chem. Soc.* **2017**, *139*, 8146. (c) Wong, A. S. Y.; Huck, W. T. S. *Beilstein J. Org. Chem.* **2017**, *13*, 1486. (d) Lehn, J.-M. *Angew. Chem., Int. Ed.* **2013**, *52*, 2836. (e) Giuseppone, N. *Acc. Chem. Res.* **2012**, *45*, 2178.

(7) (a) Kosikova, T.; Philp, D. *Chem. Soc. Rev.* **2017**, *46*, 7274. (b) Bissette, A. J.; Fletcher, S. P. *Angew. Chem., Int. Ed.* **2013**, *52*, 12800. (c) Philp, D.; Huck, J. *Supramolecular Chemistry: From Molecules to Nanomaterials*; John Wiley & Sons, Ltd.: New York, 2012; Vol. 4, p 1415. (d) Vidonne, A.; Philp, D. *Eur. J. Org. Chem.* **2009**, *2009*, 593. (e) Patzke, V.; von Kiedrowski, G. *ARKIVOC* **2007**, *46*, 293. (f) Wintner, W. A.; Conn, M. M.; Rebek, J., Jr. *Acc. Chem. Res.* **1994**, *27*, 198. (g) von Kiedrowski, G. *Bioorg. Chem. Front.* **1993**, *3*, 113.

(8) (a) Plöger, T. A.; von Kiedrowski, G. *Org. Biomol. Chem.* **2014**, *12*, 6908. (b) Lincoln, T. A.; Joyce, G. F. *Science* **2009**, *323*, 1229. (c) Kim, D.-E.; Joyce, G. F. *Chem. Biol.* **2004**, *11*, 1505. (d) Paul, N.; Joyce, G. F. *Proc. Natl. Acad. Sci. U. S. A.* **2002**, *99*, 12733. (e) Luther,

A.; Brandsch, R.; von Kiedrowski, G. *Nature* **1998**, *396*, 245. (f) Sievers, D.; von Kiedrowski, G. *Chem. —Eur. J.* **1998**, *4*, 629. (g) Sievers, D.; von Kiedrowski, G. *Nature* **1994**, *369*, 221. (h) von Kiedrowski, G.; Wlotzka, B.; Helbing, J.; Matzen, M.; Jordan, S. *Angew. Chem., Int. Ed. Engl.* **1991**, *30*, 423. (i) von Kiedrowski, G. *Angew. Chem., Int. Ed. Engl.* **1986**, *25*, 932.

(9) (a) Altay, Y.; Tezcan, M.; Otto, S. *J. Am. Chem. Soc.* **2017**, *139*, 13612. (b) Colomb-Delsuc, M.; Mattia, E.; Sadownik, J. W.; Otto, S. *Nat. Commun.* **2015**, *6*, 7427. (c) Carnall, J. M. A.; Waudby, C. A.; Belenguer, A. M.; Stuart, M. C. A.; Peyralans, J. J.-P.; Otto, S. *Science* **2010**, *327*, 1502. (d) Dadon, Z.; Wagner, N.; Ashkenasy, G. *Angew. Chem., Int. Ed.* **2008**, *47*, 6128. (e) Li, X.; Chmielewski, J. *J. Am. Chem. Soc.* **2003**, *125*, 11820. (f) Issac, R.; Chmielewski, J. *J. Am. Chem. Soc.* **2002**, *124*, 6808. (g) Yao, S.; Ghosh, I.; Zutshi, R.; Chmielewski, J. *Angew. Chem., Int. Ed.* **1998**, *37*, 478. (h) Yao, S.; Ghosh, I.; Zutshi, R.; Chmielewski, J. *Nature* **1998**, *396*, 447. (i) Severin, K.; Lee, D. H.; Kennan, A. J.; Ghadiri, M. R. *Nature* **1997**, *389*, 706. (j) Yao, S.; Ghosh, I.; Zutshi, R.; Chmielewski, J. *J. Am. Chem. Soc.* **1997**, *119*, 10559. (k) Lee, D. H.; K Granja, J. R.; Martinez, J. A.; Severin, K.; Ghadri, M. R. *Nature* **1996**, *382*, 525.

(10) (a) Sadownik, J. W.; Kosikova, T.; Philp, D. *J. Am. Chem. Soc.* **2017**, *139*, 17565. (b) Kosikova, T.; Philp, D. *J. Am. Chem. Soc.* **2017**, *139*, 12579. (c) Bottero, I.; Huck, J.; Kosikova, T.; Philp, D. *J. Am. Chem. Soc.* **2016**, *138*, 6723. (d) Dieckmann, A.; Beniken, S.; Lorenz, C. D.; Doltsinis, N. D.; von Kiedrowski, G. *Chem. — Eur. J.* **2011**, *17*, 468. (e) Kassianidis, E.; Philp, D. *Angew. Chem., Int. Ed.* **2006**, *45*, 6344. (f) Pearson, R. J.; Kassianidis, E.; Slawin, A. M. Z.; Philp, D. *Chem. — Eur. J.* **2006**, *12*, 6829. (g) Kindermann, M.; Stahl, I.; Reimold, M.; Pankau, W. M.; von Kiedrowski, G. *Angew. Chem., Int. Ed.* **2005**, *44*, 6750. (h) Wang, B.; Sutherland, I. O. *Chem. Commun.* **1997**, 1495. (i) Feng, Q.; Park, T. K.; Rebek, J., Jr. *Science* **1992**, *256*, 1179. (j) Rotello, V.; Hong, J.-I.; Rebek, J., Jr. *J. Am. Chem. Soc.* **1991**, *113*, 9422. (k) Tjivikua, T.; Ballester, P.; Rebek, J., Jr. *J. Am. Chem. Soc.* **1990**, *112*, 1249.

(11) Severin, K.; Lee, D. H.; Martinez, J. A.; Vieth, M.; Ghadiri, M. R. *Angew. Chem., Int. Ed.* **1998**, *37*, 126.

(12) (a) Kawasaki, T.; Matsumoto, A.; Sato, I.; Soai, K. Synthesis of Pyrimidine-Terminated Chiral Large Molecular Architectures with Functions of Self-Replication and Self-Improvement by Asymmetric Autocatalysis. In *Advances in Asymmetric Autocatalysis and Related Topics*; Pályi, G.; Kuri, R.; Zucchi, C. Eds.; Academic Press: Cambridge, Massachusetts, 2017, pp 149–165. (b) Saghatelian, A.; Yokobayashi, Y.; Soltani, K.; Ghadiri, M. R. *Nature* **2001**, *409*, 797.

(13) (a) Samiappan, M.; Dadon, Z.; Ashkenasy, G. *Chem. Commun.* **2011**, *47*, 710. (b) Askhenasy, G.; Dadon, Z.; Alesebi, S.; Wagner, N. *Isr. J. Chem.* **2011**, *51*, 106. (c) Allen, V. C.; Robertson, C. C.; Turega, S. M.; Philp, D. *Org. Lett.* **2010**, *12*, 1920. (d) Dadon, Z.; Samiappan, M.; Safranchik, E. Y.; Ashkenasy, G. *Chem. — Eur. J.* **2010**, *16*, 12096. (e) Ashkenasy, G.; Ghadiri, M. R. *J. Am. Chem. Soc.* **2004**, *126*, 11140.

(14) (a) Pal, A.; Malakoutikhah, M.; Leonetti, G.; Tezcan, M.; Colomb-Delsuc, M.; Nguyen, V. D.; van der Gucht, J.; Otto, S. *Angew. Chem. Int. Ed.* **2015**, *54*, 7852. (b) Rottelo, V.; Feng, Q.; Hong, J.-I.; Rebek, J., Jr. Competition, Reciprocity and Mutation at the Molecular Level: Irradiation of a Synthetic Replicator Generates a Superior Species. In *Self-Production of Supramolecular Structures*; Fleischaker, G. R.; Coonna, S.; Luisi, P. L. Eds.; NATO ASI Series (Series C: Mathematical and Physical Sciences), vol. 446; Springer: Dordrecht, 1994, pp 291–293.

(15) (a) Pieters, R. J.; Huc, I.; Rebek, J., Jr. *Tetrahedron* **1995**, *51*, 485. (b) Pieters, R. J.; Huc, I.; Rebek, J., Jr. *Angew. Chem., Int. Ed. Engl.* **1994**, *33*, 1579.

(16) (a) Kassianidis, E.; Pearson, R. J.; Wood, E. A.; Philp, D. *Faraday Discuss.* **2010**, *145*, 235. (b) Kassianidis, E.; Philp, D. *Chem. Commun.* **2006**, 4072.

(17) (a) Kosikova, T.; Hassan, N. I.; Cordes, D. B.; Slawin, A. M. Z.; Philp, D. *J. Am. Chem. Soc.* **2015**, *137*, 16074. (b) Sadownik, J. W.; Philp, D. *Angew. Chem., Int. Ed.* **2008**, *47*, 9965. (c) Pearson, R. J.; Kassianidis, E.; Slawin, A. M. Z.; Philp, D. *Org. Biomol. Chem.* **2004**, *2*, 3434. (d) Quayle, J. M.; Slawin, A. M.; Philp, D. *Tetrahedron Lett.* **2002**, *43*, 7229.

(18) Huck, J. PhD Thesis, University of St Andrews, St Andrews, **2011**.

(19) del Amo, V.; Slawin, A. M. Z.; Philp, D. *Org. Lett.* **2008**, *10*, 4589.

(20) Although imine formation is in principle reversible, the formation of imine $\mathbf{T}^{CD}$ from its constituent components (**C** and **D**) was fitted in the present work as an irreversible reaction because any attempts to fit the imine formation as a reversible process have afforded values of $k_{reverse}$ that were *ca.* 10^8 smaller than the corresponding value of $k_{forward}$ under the employed conditions (dry $CDCl_3$).

(21) Kinetic effective molarity provides a measure of the enhancement in the template-directed reaction relative to the corresponding bimolecular reaction. The parameter $EM_{kinetic}$ also provides information about the concentration at which the reaction would have to be carried out in order for the bimolecular pathway to perform with the same efficiency as the recognition-mediated pathway. As a consequence, rate acceleration is observed even if $EM_{kinetic}$ is < 1 M (as long as the concentration at which the reaction is performed is lower than $EM_{kinetic}$).

(22) In 1993, von Kiedrowski introduced[7e] the concept of catalytic efficiency (ε) and reaction order (*p*) as parameters for describing and quantifying the behavior of replicating systems. The values of kinetic effective molarity ($EM_{kinetic}$) reported in this work are not directly comparable to the values of ε reported in the literature for replicating systems. Values of $EM_{kinetic}$ are derived from the ratio of a first order rate constant and a second order rate constant and this ratio has defined units of M, hence its description as ''effective molarity''. By contrast, the parameter ε is derived from the ratio of two rate constants, one of which has units that are dependent on the value of *p*. Strictly, this parameter cannot be described as ''effective molarity'' since it

does not have units of M (unless $p = 1$) and values of ε are not strictly comparable as they most likely have different units.

(23) Thermodynamic effective molarity provides information about the stability of the template duplex relative to the strength of the ternary complex.

(24) The estimated stability of the [*trans*-$\mathbf{T^{AB} \bullet T^{CD}}$] duplex, assuming a connection EM of 1 M, is 1.2×10^7 M^{-1}. In order to determine the stability constant of this duplex experimentally using NMR, we would have to operate at concentrations centered the putative K_d, which in this case is around 100 nM. Working accurately and reproducibly at concentrations is very challenging and is complicated by the fact that dynamic processes on the NMR chemical shift timescale may start to become important at K_a values of this magnitude. Specifically, the off rate for the complex may be coincidentally similar to the frequency separation of the bound and unbound resonances. In these circumstances, the spectrum will become exchange-broadened, making analysis impossible. The compounds have no chromophores that exhibit meaningful changes on binding, thereby precluding the use of UV-vis spectroscopy.

(25) (a) Motloch, P.; Hunter, C. A. *Adv. Phys. Org. Chem.* **2016**, *50*, 77. (b) Misuraca, M. C.; Grecu, T.; Freixa, Z.; Garavini, V.; Hunter, C. A.; van Leeuwen, P. W. N. M.; Segarra-Maset, M. D.; Turega, S. M. *J. Org. Chem.* **2011**, *76*, 2723. (c) Hunter, C. A.; Anderson, H. L. *Angew. Chem., Int. Ed.* **2009**, *48*, 7488. (d) Badjić, J. D.; Nelson, A.; Cantrill, S. J.; Turnbull, W. B.; Stoddart, J. F. *Acc. Chem. Res.* **2005**, *38*, 723. (e) Hunter, C. A.; Tomas, S. *Cell Chem. Biol.* **2003**, *10*, 1023.

(26) The molecular framework that is at the core of replicator *trans*-$\mathbf{T^{AB^*}}$ has been investigated extensively by the Philp Laboratory. This autocatalytic framework shows an attenuated response to added template at levels above 20 mol% as a result of product inhibition and saturation of the catalytically-active ternary complex. See Ref. 10b for an extensive discussion.

(27) There are siginificant experimental difficulties associated with controlling the amount of water present in chlroform in a reproducible manner. Whilst it would be desirable to study the effect of the concentration of water on the rates of exchange between nitrones **B** and **B***, in practice, it was only possible to obtain reproducible results when saturating the chloroform with D_2O as described in the main text. In addition, the relative stabilities of nitrones **B** and **B*** are such that exchange occurs more readily in the direction exploited here—nitrone **B*** is considerably more stable in a hydrolytic sense than **B**, making experiments that drive the network in the opposite direction challenging.

(28) Turega, S. M.; Philp, D. *Chem. Commun.* **2006**, 3684.

(29) Padirac, A.; Fujii, T.; Estévez-Torres, A.; Rondelez, Y. J. Am. Chem. Soc. **2013**, *135*, 14586. (b) Fujii, T.; Rondelez, Y. *ACS Nano* **2013**, *7*, 27.

For Table of Contents Only: